Manuscript – article Journal of solid state chemistry, vol 226, March 2015, p. 237-242

New FCC Mg–Zr and Mg–Zr–Ti deuterides obtained by reactive milling

*Matylda N. Guzik, Stefano Deledda, Magnus H. Sørby, Volodymyr A. Yartys and Bjørn C. Hauback**

Institute for Energy Technology, P. O. Box 40, NO-2027 Kjeller, Norway

Hydrogen storage, mechanical alloying, reactive milling, metal hydrides, powder X-ray and neutron diffraction

Results for binary Mg–Zr and ternary Mg–Zr–Ti mixtures ball milled at room temperature under reactive deuterium atmosphere (5.6–6.7 MPa) are reported. X-ray and neutron powder diffraction combined with Rietveld refinements show that two new cubic phases were formed during milling. $Mg_{0.40}Zr_{0.60}D_{1.78}$ and $Mg_{0.40}Zr_{0.26}Ti_{0.34}D_{1.98}$ crystallize with disordered face centered cubic metal atom arrangements. Results of differential scanning calorimetry and termogravimetric measurements demonstrate that both deuterides desorb deuterium at lower temperatures than MgD_2, ZrD_2 or TiD_2; 528 and 575 K in the Mg–Zr–D and Mg–Zr–Ti–D system, respectively. Interestingly, $Mg_{0.40}Zr_{0.26}Ti_{0.34}D_{1.98}$ stores deuterium reversibly at 673 K and 10 MPa of D_2.

Introduction

Optimized, commercial hydrogen storage systems based on ligh-weight magnesium hydride are mainly dedicated to stationary energy storage applications[1], while on-board and small volumetric hydrogen storage solutions for portable devices are still challenging. MgH_2 contains 7.6 wt.% of hydrogen, which makes it an attractive compound for hydrogen storage applications. However, the high thermal stability and slow kinetics of its rutile-type structure significantly hinder its widespread use in commercial energy storage systems. Many factors such as a chemical composition[2-4], addition of catalytic species[5-10], processing technologies[5, 11-14] and microstructural parameters, particularly grain size[6, 15-17], have an effect on the hydrogen storage capacity, kinetics and/or thermodynamics of Mg-based intermetallic compounds. Conventional crystalline alloys often suffer from relatively slow hydrogen sorption kinetics even at high temperatures, while nanocrystalline and amorphous materials exhibit much faster kinetics at lower temperatures, as their large number of interfaces, defects and grain boundaries, provide easy pathways for hydrogen diffusion[18-21]. Their wider use is however limited by the poor reversibility at ambient temperature and pressure. In recent years, many investigations have therefore explored different ways that could efficiently reduce the hydrogen sorption temperatures and improve the reversibility of Mg-based metal hydrides. Several approaches, e.g. elemental substitutions[22-26] , mechanical alloying[22, 25, 27] and high-pressure synthesis[28], have been applied separately or jointly resulting in a formation of a number of improved and promising compounds but none of them reveal outstanding kinetic or/and thermodynamic properties. Novel Mg–TM hydrides (TM = transition metal) have been previously obtained from MgH_2 and different TM or TM hydrides in an anvil cell under mechanical pressure of several GPa[29]. This technique was successfully used for Mg-based hydrides with Hf[28, 30-31], Nb[28, 31-34], Mo[34], Ta[28, 30-

[31], Ti[28-29, 35], V[28] and Zr[28, 30-31, 34, 36]. All compounds, except a fully disordered Zr-containing phase, crystallize with face-centered cubic (FCC) metal atom arrangement that can be described as Ca_7Ge-type structure with hydrogen atoms located in two different tetrahedral sites[28 and references therein]. The presence of the TM atoms helps to retain the cubic structure of hydrides when releasing the high pressure down to ambient. Unfortunately, upon heating, most of the resulting Mg-TM hydrides decompose to binary hydrides releasing gaseous hydrogen at temperatures 100–150 K below pure MgH_2[30, 32-33, 37]. Formation of monoclinic phases, e. g. $Mg_{0.33}Zr_{0.67}H_{\sim 2}$ and $Mg_{0.33}Nb_{0.67}H_{\sim 2}$, which are thermally more stable than cubic ones, have been reported for certain TMs (Nb, Zr, Hf and Ta)[31]. $Mg_{0.82}Zr_{0.18}H_2$ obtained at high pressure can reversibly release ~ 3.0–3.5 wt. % of H_2 (i.e. 60–70% of the total hydrogen content) at 523 K[36]. The FCC structure of the hydride is preserved due to remaining hydrogen, which most likely stabilizes the metastable phase[30, 36]. The same behavior has been reported for disorder FCC Ti-containing Mg-based hydrides[23-24]. In spite of being thermodynamically immiscible, extended solubility of Mg in Ti and *vice versa* has been achieved by mechanical milling[38-40 and references therein]. It has been reported that $Mg_{1-y}Ti_y$ intermetallic compounds ($0.2 < y < 0.65$) can crystallize either with FCC, body-centered cubic (BCC) or hexagonal close-packed (HCP) structure depending on the elemental composition of the starting mixture as well as the dynamic energy delivered by the milling media[41]. Partial substitution of Mg atoms by Ti atoms is expected to preserve the cubic structure of Mg–Ti hydride during hydrogen cycling and decrease sorption temperature. Single Mg–Ti–H phase with up to 4.0 wt % of H_2 can be formed from mechanically alloyed powder at 423 K under 8 MPa of hydrogen gas[42-43]. However, hydrogenation of Ti/Mg solid solutions at 563 K can result in their decomposition to MgH_2 and TiH_2[44-45]. In this paper we focus on alloying Mg–Zr and Mg–Zr–Ti powder mixtures under deuterium gas and report on the

synthesis, structural characterization and thermal stability of deuterides obtained by reactive ball milling. The results are compared to published data for Mg–Zr hydrides[36] obtained by high-pressure synthesis. Single-phase deuterides in the Mg–Zr–Ti system have not been reported previously.

Synthesis and characterization

Elemental powder mixtures with nominal composition $Mg_{0.45}Zr_{0.55}$ and $Mg_{0.45}Zr_{0.25}Ti_{0.30}$ (all metals purchased from Alfa Aesar, purity of 99% or better), were ball milled under a reactive atmosphere of deuterium gas, 5.6 and 6.7 MPa, respectively, in a commercial vial from evicomagnetics[46]. This specially designed hardened steel vial, equipped with pressure and temperature sensors, is compatible with the Fritsch P6 planetary ball mill. Milling was carried out at 450 rpm for 24 hours with ball-to-powder weight ratio of 40:1. Deuterium gas was used instead of natural hydrogen for powder neutron diffraction (PND) experiments. The powders were handled in a glove box under protective Ar atmosphere (< 0.1 ppm O_2 and H_2O). The as-milled powders were analyzed by both high resolution synchrotron powder X-ray diffraction (SR-PXD) as well as PND. SR-PXD measurements were performed at the Swiss-Norwegian beam line (SNBL), ESRF (Grenoble, France), at the BM01B station. The wavelengths for the experiments where: λ = 0.50350 and 0.50462 Å. In all SR-PXD experiments the powders were sealed in boron-glass capillaries (d = 0.3 mm). PND data were collected with the PUS diffractometer (λ = 1.5557 Å) at the JEEP II reactor (Kjeller, Norway). The samples were loaded into 6 mm vanadium container and sealed with indium wire. Rietveld refinements were performed with the software *FULLPROF*[47]. X-ray scattering factors and neutron cross-sections were taken from the *FULLPROF* library. The SR-PXD backgrounds were modeled by Chebyshev polynomials, while 12-coefficient Fourier-cosine polynomial was used to fit the

background in the PND data. In both cases Fourier filtering procedure was applied at the final stages of the refinements. Pseudo-Voigt profile function was used to model the Bragg peak shapes. Deuterium desorption was investigated by differential scanning calorimetry (DSC), thermogravimetric analysis (TG) and temperature programmed desorption (TPD). DSC and TG measurements were carried out using *NETSCH* STA449C Jupiter instrument at 5 K/min in argon flow (50 ml/min). TPD experiments were performed in an in-house built setup and carried out under dynamic vacuum using heating rates of 5 K/min. Gas desorption was detected as a temporary increase of the pressure in the system. Elemental analysis was performed in the Hitachi S–4800 scanning electron microscope (SEM) equipped with the Noran System Six energy dispersive spectrometer (EDS). Absorption/desorption experiments were performed using an in-house built Sieverts apparatus equipped with a pressure sensor from Presens[48] operable up to 20 MPa and 773 K.

Results

Synthesis by reactive milling

Figure 1 presents the changes of pressure and temperature during ball milling of 0.45 Mg + 0.55 Zr and 0.45 Mg + 0.25 Zr + 0.30 Ti (molar ratio) powder mixtures in D_2 atmosphere. In both cases the temperature increases sharply in the early stage of the milling and reaches a value of 320 K after 3 hours. Such behavior is typical for planetary ball milling and results from the impact and attrition of the balls on the internal walls of the vial. For both mixtures, a significant increase of pressure at the beginning of milling is also observed, which is consistent with the temperature rise. A decrease of the pressure is recorded after approx. 100 and 15 min of milling for Mg–Zr and Mg–Zr –Ti mixture, respectively, and can be assigned to the onset of deuterium

absorption. The formation of deuteride phases, induced by the mechanical transformation, occurs in one step and is significantly faster in the Ti-containing sample. A small hump appearing on the pressure curve between 4 and 5 hours of milling is most likely related to the observed temperature variation. The influence of Ti content in the ball milled mixture on the kinetics of hydrogen absorption reaction has already been reported[17, 38-40, 49-52]. Since the reaction appears to proceed in a single step, it seems unlikely that formation of TiD_2 as intermediate product is the cause of accelerated formation of the final deuteride. However, the abrasive role of the possible Ti–D-based phase that can promote deuterium uptake in Mg–Zr powder cannot be excluded[38-40]. After 4 and 2 hours of milling the deuterium absorption significantly slows down and no notable changes of pressure are observed after 10 and 8 hours of milling for Mg–Zr and Mg–Zr–Ti powder mixture, respectively.

X-ray and neutron diffraction

Joint Rietveld refinements performed on the PND and SR-PXD data indicate that both the Mg–Zr–D and the Mg–Zr–Ti–D samples, after 24 hours of reactive ball milling, are dominated by a phase that crystallizes with FCC metal atoms arrangement (space group: *Fm*-3*m*). The obtained fits are shown in Figure 2. In the Mg–Zr-containing sample, the main cubic phase accounts for 90 wt. %. Apart from that, traces of MgO (most likely originated from starting Mg metal powder)[53], Fe (milling media debris) and ZrD_x are confirmed. No peaks from MgD_2 are observed. The as-milled Mg–Zr–Ti powder consists of 97 wt.% of the FCC phase and 3 wt.% of MgO. The quite broad diffraction peaks are typical for ball milled powders and indicate a nanocrystalline microstructure. The refined lattice parameter of the obtained ternary cubic deuteride in Mg–Zr–D system is a = 4.7730(8) Å (V = 108.73(3) $Å^3$). This value is very close to the experimental one for the pure cubic phase of ZrH_2 (a = 4.777 Å), however it is also expected

for the substituted Mg–Zr–D phase, due to the same values of atomic radii for Mg and Zr, 1.602 Å[54]. Apart from this, the lack of peaks that could be ascribed to the magnesium deuteride or other magnesium-containing phases, besides the minor MgO impurities, indicates that the formation of the ternary phase indeed took place. Due to the simplicity of the cubic structure that can cause strong correlations among refined parameters, the Rietveld refinements were carried out with a constrained occupancy factor on the metal site (Wyckoff position *4a*). The molar metal atoms (Mg/Zr) ratio was fixed according to the results obtained from the sample elemental analysis (Mg/Zr = 0.40/0.60), which suggested a slightly higher amount of Zr compared to the nominal composition (Mg/Zr = 0.45/0.55). The occupancy factor for D atoms on the tetrahedral site (*8c*) was also refined. The obtained value, n = 0.89(1), suggests that tetrahedral interstitial holes are occupied almost completely by D atoms. There is no indication of deuterium atoms in the octahedral interstices. In total, 27 parameters were allowed to vary during the final refinement: 8 scale factors, 2 zero shift, 12 profile and 1 unit cell parameter, 2 isotropic displacement parameters and 1 occupancy factor (for deuterium atoms). The overall refined composition of the synthesized ternary deuteride is $Mg_{0.40}Zr_{0.60}D_{1.78(1)}$. The value for the cell volume per formula unit obtain from Rietveld refinements is $V_{Rietveld}$/f.u. = 27.16 Å^3. This is in a good agreement with the theoretical value $V_{theoretical}$/f.u. = 28.68 Å^3, which is estimated by linearly combining the cell volume per formula unit for pure MgD_2 (30.80 Å^3) and ZrD_2 (27.79 Å^3), scaled by 0.40 and 0.60, respectively. This small deviation could possibly result from a lower concentration of deuterium in the synthesized $Mg_{0.40}Zr_{0.60}D_{1.78(1)}$ and/or presence of lattice strains that is known to reduce deuterium content in metal hydrides[55-56]. For the Mg–Zr–Ti system, combined Rietveld refinements with PND and SR-PXD data were also carried out with a constrained molar ratio of metal atoms according to the sample elemental analysis results

(Mg/Zr/Ti = 0.40/0.26/0.34) which confirmed the relatively close composition of the as-milled phase to the nominal values of the starting mixture (Mg/Zr/Ti = 0.45/0.25/0.30). The refined occupancy factor of the deuterium site (*8c*), n = 0.99(1), suggests an ordered distribution of deuterium atoms over tetrahedral interstitial sites. Similar to the Mg–Zr sample there are no indications about presence of D atoms in octahedral sites. In total, 22 parameters were refined: 4 scale factors, 2 zero shift, 12 profile, 1 unit cell parameter, 2 isotropic displacement parameters and 1 occupancy factor (for deuterium atoms). The refined composition of the quaternary deuteride is $Mg_{0.40}Zr_{0.26}Ti_{0.34}D_{1.98(1)}$ with unit cell parameter a = 4.6419(9) Å (V = 100.02(3) $Å^3$). Furthermore, the cell volume per formula unit value obtained from the refinement, $V_{Rietveld}$/f.u. = 25.58 $Å^3$, is in a good agreement with the theoretical value ($V_{theoretical}$/f.u. = 26.80$Å^3$). SR-PXD and PND data clearly show that the planetary ball milling under deuterium gas pressure has led to the formation of TM-based metal deuterides. Only one of those deuterides has been previously synthesized by the ultra-high GPa technique. Synthesis conditions and summary of Rietveld refinements are listed in Table 1.

Table 1. Summary of crystal structures, lattice parameters, synthesis and reversible hydrogen/deuterium storage conditions for selected hydrides/deuterides.

Phase composition	**Space group**	**Unit cell parameter *a* (Å)**	**Synthesis method and conditions**	**Reversible hydrogen/deuterium storage conditions**
$Mg_{0.40}Zr_{0.60}D_{1.78}$	*Fm-3m*	4.7730(8)	reactive milling under D_2 gas, T = 298 K, p = 5.6 MPa	-
$Mg_{0.40}Zr_{0.26}Ti_{0.34}D_{1.98}$	*Fm-3m*	4.6419(9)	reactive milling under D_2 gas, T = 298 K, p = 6.7 MPa	T = 673 K p = 10 MPa
$Mg_{0.25}Ti_{0.75}H_{1.62}$ [43]	*Fm-3m*	4.4565(5)	hydrogenation of ball milled alloy, T = 423 K, p = 8 MPa	-
$Mg_{0.82}Zr_{0.18}H_2$ [36]	*Fm-3m*	4.8712(2)	Synthesis in an anvil cell from metal hydrides, T = 423 K, p = 8GPa	T = 573 K p = 0.5 MPa

D-storage properties and thermal stability of the deuterides

The deuterium desorption behaviors of $Mg_{0.40}Zr_{0.60}D_{1.78}$ and $Mg_{0.40}Zr_{0.26}Ti_{0.34}D_{1.98}$ were investigated by DSC. During experiments both samples were heated up to 873 K with an increment of 5 K/min and cooled down to room temperature. Figure 3 shows the DSC scans for the as-milled deuterides. A single-step desorption around 530 K is observed for the Mg–Zr-based deuteride. This is far below the desorption temperature of ZrD_2 (about 800 K) and confirms the presence of Mg in the FCC structure. The obtained ternary deuteride appears also to be less stable than previously reported Mg–Zr hydrides[30, 36], for which the onset temperature of the dominant peak was observed at 543 K (TPD, the heating rate 10K/min under vacuum). In this study, $Mg_{0.40}Zr_{0.60}D_{1.78}$ the onset temperature for desorption was at 476 K (DSC, the heating rate 5K/min under argon flow). The desorption for $Mg_{0.40}Zr_{0.26}Ti_{0.34}D_{1.98}$ starts at 497 K and shows a maximum at ~575 K. The measured mass losses, ascribed to the release of deuterium gas, are 1.95 and 2.96 wt.% for $Mg_{0.40}Zr_{0.60}D_{1.78}$ and $Mg_{0.40}Zr_{0.26}Ti_{0.34}D_{1.98}$, respectively. It is worth noticing that the presence of Ti in the structure increases the peak of desorption temperature by ~50 K. One could expect that by introducing Ti, which forms less stable hydride than Zr, and keeping the same amount of Mg, the quaternary deuteride should desorb deuterium at lower temperatures than $Mg_{0.40}Zr_{0.60}D_{1.78}$. Since it is not the case, there must be governing factors other than the stabilities of corresponding binary hydrides, which influence the sorption temperature of the compounds. One of the possibilities is negative value of metal– deuterium mixing enthalpies for a given deuterium concentration that could increase D bonding in the deuteride and cause its reversibility, as predicted by theoretical calculations[57] and presented below experimentally. These aspects of thermodynamics, but also kinetics, require further dedicated studies. After heating to 873 K in the DSC, the powders were studied by SR-PXD at room temperature (Figure

4). In the Mg–Zr-based sample FCC $Mg_{0.40}Zr_{0.60}D_x$ is the main phase (50 wt.%). It retains its cubic structure but with a smaller unit cell volume, V = 108.45(2) Å^3, a = 4.7685(5) Å. Shrinking of the cell parameter suggests a partial release of deuterium from $Mg_{0.40}Zr_{0.60}D_{1.78}$. Nevertheless, during heating, new phases are formed, indicating that desorption also results from the partial decomposition of the deuterated phase. The SR-PXD data analysis confirms presence of elemental Mg (37 wt.%) , MgO (5 wt.%) and Fe (3 wt.%) as well as $ZrFe_2$ (5 wt.%). DSC measurement of the Mg–Zr–Ti deuteride results in phase decomposition to a much greater extend. The sample contains only 16 wt. % of the FCC phase after heating to 873 K. Its refined unit cell parameter, a = 4.7571(5) Å, is much larger than that for the FCC deuteride observed in the as-milled sample (4.6419(9) Å) and similar to the value observed for the desorbed Mg–Zr deuteride (a = 4.7685(5) Å). This could suggest that Ti atoms, with the smallest atomic radius (1.47 Å)[54], "leak" from the cubic phase and take part in formation of new phases. This scenario is supported by the presence of Mg (34 wt.%), $ZrTi_2D_4$ (46 wt.%) and MgO (4 wt.%) in the sample after the DCS measurement. Assuming a stoichiometric reaction for Zr and Ti atoms during the heating, one can calculate a composition of the FCC deuteride, which is $Mg_{0.58}Zr_{0.28}Ti_{0.16}D_{\sim 1.98}$

Reversible D-storage in $Mg_{0.40}Zr_{0.26}Ti_{0.34}D_{1.98}$

Mg-based hydrides are often unstable and highly reactive with a tendency to form new phases at elevated temperature. Thus, the TPD experiment for $Mg_{0.40}Zr_{0.26}Ti_{0.34}D_{1.98}$ was carried out at lower temperatures than DSC ones (up to 873 K). The sample was heated up to 673 K at 5 K/min under dynamic vacuum and subsequently cooled down. Afterwards, the powder was investigated by means of high resolution SR-PXD. Figure 5 shows the fit obtained by Rietveld refinements. Contrary to the observations after DCS measurement, the sample consists of two FCC phases,

FCC_1 (26 wt.%) and FCC_2 (32 wt.%), with different refined lattice constants, a_{FCC1} = 4.643(7), a_{FCC2} = 4.553(1) Å, respectively. MgO and elemental Mg are also observed. The SR-PXD pattern was refined using the structure model of the as-milled deuteride with respect to symmetry (space group *Fm*-3*m*) and metal atoms ratio as the starting point for both cubic phases. The unit cell parameter of the FCC_1 phase is within the estimated standard deviation range of the value calculated for the as-milled $Mg_{0.40}Zr_{0.26}Ti_{0.34}D_{1.98}$ (a = 4.6419(9) Å) and suggests that upon heating up to 673 K the metal lattice of the deuteride does not decompose as observed during the DSC experiment. The second phase, FCC_2, differs from FCC_1 only by the value of the lattice constant. It indicates that $Mg_{0.40}Zr_{0.26}Ti_{0.34}D_{1.98}$, when heated up under dynamic vacuum to 673 K, preserves its structure while partially releasing deuterium. This results in the formation of a cubic phase with a smaller unit cell dimension and lower deuterium content. The presence of elemental Mg phase can be explained by the partial sample decomposition. To explore the reversibility of $Mg_{0.40}Zr_{0.26}Ti_{0.34}D_{1.98}$, the desorbed sample was again heated up to 673 K under dynamic vacuum, loaded with 10 MPa of D_2 gas for 18 hours, and then cooled down to room temperature. The resulting powder was studied by high resolution SR-PXD. The data after Rietveld refinement are presented in Figure 5. It can be clearly seen that after re-deuteration the powder consists, beside a small fraction of MgO, of just one FCC phase with a refined lattice parameter a = 4.634(3) Å. This value is only slightly smaller than the one found for the as-milled $Mg_{0.40}Zr_{0.26}Ti_{0.34}D_{1.98}$ and indicates that in $Mg_{0.40}Zr_{0.26}Ti_{0.34}D_{1.98}$ deuterium desorption/absorption is reversible at 673 K. Since the re-deuterated cubic phase shows a smaller unit cell, one can expect a slightly reduced deuterium storage capacity. At the same time, because of the large peak width in the re-deuterated sample, it cannot be excluded that there is more than one crystalline

cubic or/and MgD_2 phase present. However, due to the inherent nature of the powder, they are impossible to be distinguished.

Conclusions

The syntheses of deuterides in the Mg–Zr–D and Mg–Zr–Ti–D systems by reactive milling in deuterium atmosphere have been explored, together with their deuterium storage properties. The combined Rietveld refinements performed on SR-PXD and PND data confirm the formation of new FCC deuterated phases with refined deuterium contents of $Mg_{0.40}Zr_{0.60}D_{1.78}$ and $Mg_{0.40}Zr_{0.26}Ti_{0.34}D_{1.98}$, respectively. Both compounds release deuterium gas at temperatures 120–180 K lower than pure MgD_2 and previously reported $Mg_{0.82}Zr_{0.18}D_2$ prepared by ultra-high GPa hydrogen pressure method. The amount of desorbed D_2 gas accounts for 1.95 wt.% and 2.96 wt.% for $Mg_{0.40}Zr_{0.60}D_{1.78}$ and $Mg_{0.40}Zr_{0.26}Ti_{0.34}D_{1.98}$, respectively. The quaternary deuteride obtained in Mg–Zr–Ti–D system reveals reversible deuterium storage behavior at 673 K and 10 MPa of D_2. High-resolution SR-PXD data show that the FCC structure of $Mg_{0.40}Zr_{0.26}Ti_{0.34}D_{1.98}$ is preserved during deuterium desorption/absorption cycle without a significant phase segregation. The FCC phase fraction in the re-deuterated sample is estimated to be ~95 wt.%, however the unit cell parameter of the re-deuterated phase is slightly smaller (Δa = 0.2 %) than the one found for the as-milled phase.

FIGURES

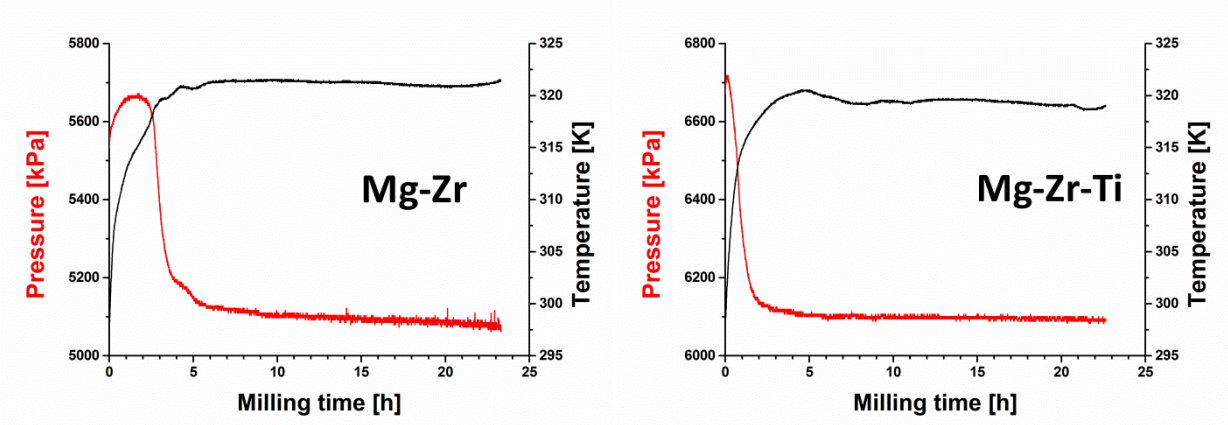

a) b)

Figure 1. Pressure (red) and temperature (black) inside the vial plotted as a function of the milling time for Mg-Zr (a) and Mg-Zr-Ti (b) powder mixtures ball milled in D2.

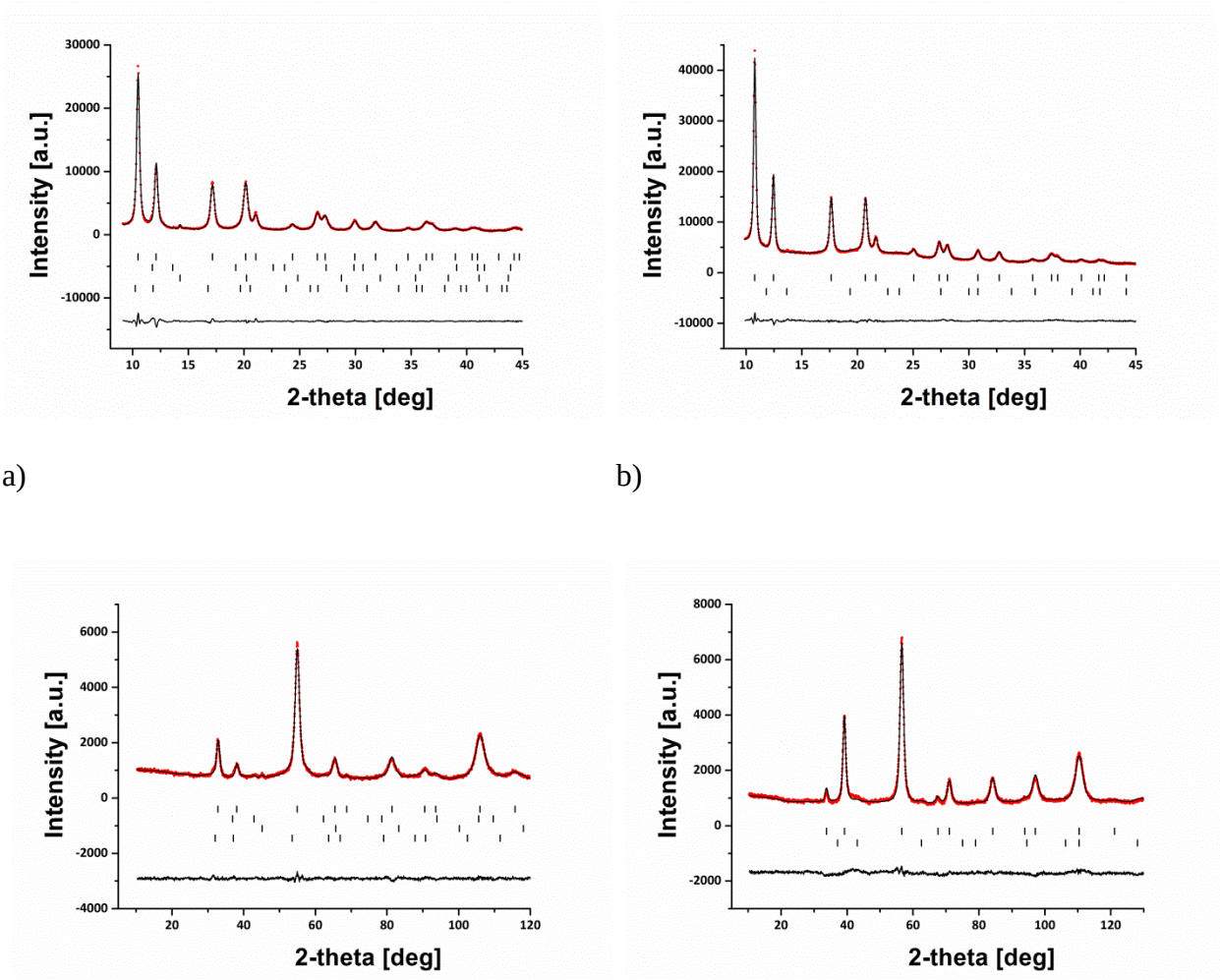

Figure 2. Observed (red line), calculated (black line) and difference (bottom line) high resolution SR-PXD (a, b) and PND (c, d) patterns obtained for $Mg_{0.40}Zr_{0.60}D_{1.78}$ (a, c) and $Mg_{0.40}Zr_{0.26}Ti_{0.34}D_{1.98}$ (b, d). Vertical bars indicate Bragg peaks positions of contributing phases, from top to bottom: $Mg_{0.40}Zr_{0.60}D_{1.78}$, MgO, Fe, ZrD_x (a, c); $Mg_{0.40}Zr_{0.26}Ti_{0.34}D_{1.98}$, MgO (b, d).

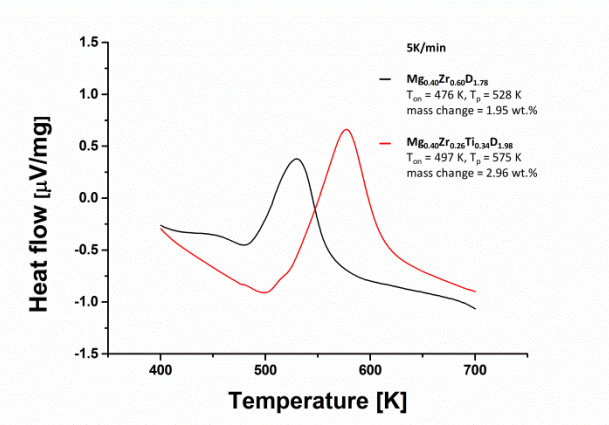

Figure 3. DSC scans (5 K/min) for as-milled $Mg_{0.40}Zr_{0.60}D_{1.78}$ (black) and $Mg_{0.40}Zr_{0.26}Ti_{0.34}D_{1.98}$ (red).

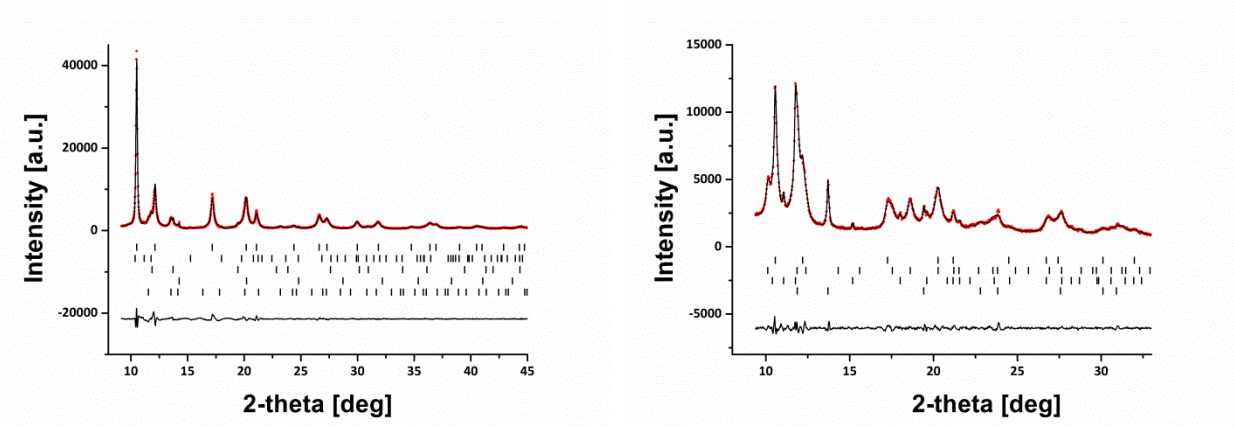

a) b)

Figure 4. Observed (red line), calculated (black line) and difference (bottom line) high resolution SR-PXD patterns obtained for $Mg_{0.40}Zr_{0.60}D_{1.78}$ (a) and $Mg_{0.40}Zr_{0.26}Ti_{0.34}D_{1.98}$ (b) after DSC measurements. Vertical bars indicate Bragg peaks positions of contributing phases, from top to bottom: FCC, MgO, Fe, $ZrFe_2$ (a); FCC, $ZrTi_2D_4$, Mg, MgO (b).

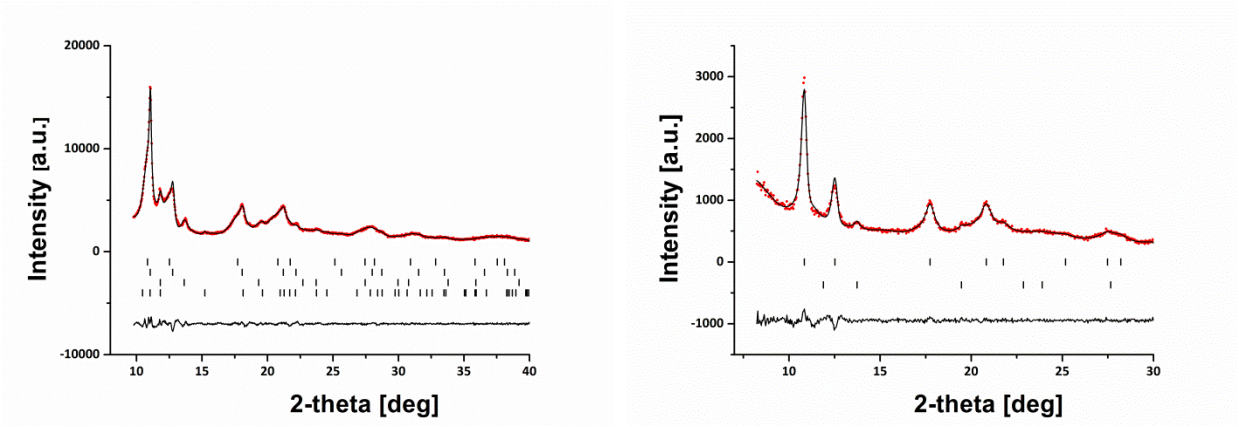

a) b)

Figure 5. Observed (red line), calculated (black line) and difference (bottom line) high resolution SR-PXD patterns obtained for $Mg_{0.40}Zr_{0.26}Ti_{0.34}D_{1.98}$ after desorption in vacuum (a) and reabsorption under 10 MPa of D_2 (b) at 673 K. Vertical bars indicate Bragg peaks positions of contributing phases, from top to bottom: FCC_1, FCC_2, MgO, Mg (a); FCC, MgO (b).

Corresponding Author

* Physics Department, Institute for Energy Technology, PO Box 40, NO-2027 Kjeller, Norway. Fax: +47 6381 0920; Tel.: +47 974 08 844; E-mail: bjorn.hauback@ife.no

Acknowledgements

This work was supported by the Norwegian Research Council under the NANOMAT project no. 203323 “Novel Mg-based Materials for Advanced Ni-Metal Hydride Batteries”.

References

(1) Jehan, M.; Fruchart, D. McPhy-Energy's Proposal for Solid State Hydrogen Storage Materials and Systems. *J Alloy Compd* **2013**, *580*, S343–S348.
(2) Selvam, P.; Viswanathan, B.; Swamy, C. S.; Srinivasan, V. Magnesium and Magnesium Alloy Hydrides. *Int J Hydrogen Energy* **1986**, *11*, 169–192.
(3) Bogdanovic, B.; Hofmann, H.; Neuy, A.; Reiser, A.; Schlichte, K.; Spliethoff, B.; Wessel, S. Ni-Doped versus Undoped Mg-MgH_2 Materials for High Temperature Heat or Hydrogen Storage. *J Alloy Compd* **1999**, *292*, 57–71.
(4) Liang, G.; Huot, J.; Boily, S.; Van Neste, A.; Schulz, R. Hydrogen Storage Properties of Nanocrystalline $Mg_{1.9}Ti_{0.1}Ni$ Made by Mechanical Alloying. *J Alloy Compd* **1999**, *282*, 286–290.
(5) Liang, G.; Huot, J.; Boily, S.; Van Neste, A.; Schulz, R. Catalytic Effect of Transition Metals on Hydrogen Sorption in Nanocrystalline Ball Milled MgH_2-TM (TM=Ti, V, Mn, Fe and Ni) Systems. *J Alloy Compd* **1999**, *292*, 247–252.
(6) Barkhordarian, G.; Klassen, T.; Bormann, R. Catalytic Mechanism of Transition-Metal Compounds on Mg Hydrogen Sorption Reaction. *J Phys Chem B* **2006**, *110*, 11020–11024.
(7) Hanada, N.; Ichikawa, T.; Fujii, H. Catalytic Effect of Ni Nano-Particle and Nb Oxide on H-Desorption Properties in MgH_2 Prepared by Ball Milling. *J Alloy Compd* **2005**, *404*, 716–719.
(8) Hanada, N.; Ichikawa, T.; Fujii, H. Catalytic Effect of Nanoparticle 3d-Transition Metals on Hydrogen Storage Properties in Magnesium Hydride MgH_2 Prepared by Mechanical Milling. *J Phys Chem B* **2005**, *109*, 7188–7194.
(9) Hanada, N.; Ichikawa, T.; Fujii, H. Catalytic Effect of Niobium Oxide on Hydrogen Storage Properties of Mechanically Ball Milled MgH_2. *Physica B* **2006**, *383*, 49–50.
(10) Tonus, F.; Fuster, V.; Urretavizcaya, G.; Castro, F. J.; Bobet, J. L. Catalytic Effect of Monoclinic WO_3, Hexagonal WO_3 and $H_{0.23}WO_3$ on the Hydrogen Sorption Properties of Mg. *Int J Hydrogen Energy* **2009**, *34*, 3404–3409.
(11) Huot, J.; Ravnsbæk, D. B.; Zhang, J.; Cuevas, F.; Latroche, M.; Jensen, T. R. Mechanochemical Synthesis of Hydrogen Storage Materials. *Prog Mater Sci* **2013**, *58*, 30–75.
(12) Huot, J.; Liang, G.; Boily, S.; Van Neste, A.; Schulz, R. Structural Study and Hydrogen Sorption Kinetics of Ball-Milled Magnesium Hydride. *J Alloy Compd* **1999**, *293*, 495–500.
(13) Liang, G.; Huot, J.; Boily, S.; Van Neste, A.; Schulz, R. Hydrogen Storage Properties of the Mechanically Milled MgH_2-V Nanocomposite. *J Alloy Compd* **1999**, *291*, 295–299.
(14) Schulz, R.; Huot, J.; Liang, G.; Boily, S.; Lalande, G.; Denis, M. C.; Dodelet, J. P. Recent Developments in the Applications of Nanocrystalline Materials to Hydrogen Technologies. *Mat Sci Eng A-Struct* **1999**, *267*, 240–245.
(15) Barkhordarian, G.; Klassen, T.; Bormann, R. Kinetic Investigation of the Effect of Milling Time on the Hydrogen Sorption Reaction of Magnesium Catalyzed with Different Nb_2O_5 Contents. *J Alloy Compd* **2006**, *407*, 249–255.
(16) Imamura, H.; Masanari, K.; Kusuhara, M.; Katsumoto, H.; Sumi, T.; Sakata, Y. High Hydrogen Storage Capacity of Nanosized Magnesium Synthesized by High Energy Ball-Milling. *J Alloy Compd* **2005**, *386*, 211–216.
(17) Aguey-Zinsou, K. F.; Fernandez, J. R. A.; Klassen, T.; Bormann, R. Effect of Nb_2O_5 on MgH_2 Properties During Mechanical Milling. *Int J Hydrogen Energy* **2007**, *32*, 2400–2407.
(18) Kim, H. J.; Nakamura, J.; Shao, H. Y.; Nakamura, Y.; Akiba, E.; Chapman, K. W.; Chupas, P. J.; Proffen, T. Variation in the Ratio of Mg_2Co and $MgCo_2$ in Amorphous-Like Mechanically

Alloyed Mg_xCo_{100-x} Using Atomic Pair Distribution Function Analysis. *Z Kristallogr* **2012**, *227*, 299–303.
(19) Shao, H. Y.; Asano, K.; Enoki, H.; Akiba, E. Preparation and Hydrogen Storage Properties of Nanostructured Mg-Ni BCC Alloys. *J Alloy Compd* **2009**, *477*, 301–306.
(20) Shao, H. Y.; Asano, K.; Enoki, H.; Akiba, E. Fabrication, Hydrogen Storage Properties and Mechanistic Study of Nanostructured $Mg_{50}Co_{50}$ Body-Centered Cubic Alloy. *Scripta Mater* **2009**, *60*, 818–821.
(21) Shao, H. Y.; Asano, K.; Enoki, H.; Akiba, E. Correlation Study Between Hydrogen Absorption Property and Lattice Structure of Mg-Based BCC Alloys. *Int J Hydrogen Energy* **2009**, *34*, 2312–2318.
(22) Chen, D.; Wang, Y. M.; Chen, L.; Liu, S.; Ma, C. X.; Wang, L. B. Alloying Effects of Transition Metals on Chemical Bonding in Magnesium Hydride MgH_2. *Acta Mater* **2004**, *52*, 521–528.
(23) Kalisvaart, W. P.; Notten, P. H. L. Mechanical Alloying and Electrochemical Hydrogen Storage of Mg-Based Systems. *J Mater Res* **2008**, *23*, 2179–2187.
(24) Kalisvaart, W. P.; Wondergem, H. J.; Bakker, F.; Notten, P. H. L. Mg-Ti Based Materials for Electrochemical Hydrogen Storage. *J Mater Res* **2007**, *22*, 1640–1649.
(25) Pauw, B. R.; Kalisvaart, W. P.; Tao, S. X.; Koper, M. T. M.; Jansen, A. P. J.; Notten, P. H. L. Cubic MgH_2 Stabilized by Alloying with Transition Metals: a Density Functional Theory Study. *Acta Mater* **2008**, *56*, 2948–2954.
(26) Cuevas, F.; Fernandez, J. F.; Ares, J. R.; Leardini, F.; Latroche, M. Crystal Structure and Hydrogenation Properties of Pseudo-Binary $Mg_6Pd_{0.5}Ni_{0.5}$ Complex Metallic Alloy. *J Solid State Chem* **2009**, *182*, 2890–2896.
(27) Er, S.; Tiwari, D.; de Wijs, G. A.; Brocks, G. Tunable Hydrogen Storage in Magnesium-Transition Metal Compounds: First-Principles Calculations. *Phys Rev B* **2009**, *79*, 024105–024108.
(28) Moser, D.; Bull, D. J.; Sato, T.; Noreus, D.; Kyoi, D.; Sakai, T.; Kitamura, N.; Yusa, H.; Taniguchi, T.; Kalisvaart, W. P.; Notten, P. Structure and Stability of High Pressure Synthesized Mg-TM hydrides (TM = Ti, Zr, Hf, V, Nb and Ta) as Possible New Hydrogen Rich Hydrides for Hydrogen Storage. *J Mater Chem* **2009**, *19*, 8150–8161.
(29) Kyoi, D.; Sato, T.; Ronnebro, E.; Kitamura, N.; Ueda, A.; Ito, M.; Katsuyama, S.; Hara, S.; Noreus, D.; Sakai, T. A New Ternary Magnesium-Titanium Hydride Mg_7TiH_x with Hydrogen Desorption Properties Better than Both Binary Magnesium and Titanium Hydrides. *J Alloy Compd* **2004**, *372*, 213–217.
(30) Kyoi, D.; Sakai, T.; Kitamura, N.; Ueda, A.; Tanase, S. Synthesis of FCC Mg-Zr and Mg-Hf Hydrides Using GPa Hydrogen Pressure Method and Their Hydrogen-Desorption Properties. *J Alloy Compd* **2008**, *463*, 311–316.
(31) Okada, M.; Goto, Y.; Kataoka, R.; Yambe, Y.; Kamegawa, A.; Takamura, H. Novel Hydrides in Mg-TM Systems Synthesized by High Pressure (TM = Zr, Nb, Hf and Ta). *J Alloy Compd* **2007**, *446*, 6–10.
(32) Sato, T.; Kyoi, D.; Ronnebro, E.; Kitamura, N.; Sakai, T.; Noreus, D. Structural Investigations of Two New Ternary Magnesium-Niobium Hydrides, $Mg_{6.5}NbH_{\sim 14}$ and $MgNb_2H_{\sim 4}$. *J Alloy Compd* **2006**, *417*, 230–234.
(33) Kyoi, D.; Kitamura, N.; Tanaka, H.; Ueda, A.; Tanase, S.; Sakai, T. Hydrogen Desorption Properties of FCC Super-Lattice Hydride Mg_7NbH_x Prepared by Ultra-High Pressure Techniques. *J Alloy Compd* **2007**, *428*, 268–273.

(34) Goto, Y.; Hayashi, T.; Kataoka, R.; Kakuta, H.; Kamegawa, A.; Takamura, H.; Okada, M. High-Pressure Synthesis of Novel Hydrides in Mg-TM Systems (TM = Zr, Nb and Mo). *Mater Trans* **2005**, *46*, 1798–1801.
(35) Ronnebro, E.; Kyoi, D.; Kitano, A.; Kitano, Y.; Sakai, T. Hydrogen Sites Analysed by X-Ray Synchrotron Diffraction in Mg_7TiH_{13-16} Made at Gigapascal High-Pressures. *J Alloy Compd* **2005**, *404*, 68–72.
(36) Takasaki, T.; Kyoi, D.; Kitamura, N.; Tanase, S.; Sakai, T. Reversible Hydrogen Storage Property and Structural Analysis for Face-Centered Cubic Hydride $Mg_{0.82}Zr_{0.18}H_2$ Prepared by Gigapascal Hydrogen Pressure Method. *J Phys Chem B* **2007**, *111*, 14102–14106.
(37) Kyoi, D.; Sakai, T.; Kitamura, N.; Ueda, A.; Tanase, S. Synthesis of FCC Mg-Ta Hydrides Using GPa Hydrogen Pressure Method and Their Hydrogen-Desorption Properties. *J Alloy Compd* **2008**, *463*, 306–310.
(38) Cuevas, F.; Korablov, D.; Latroche, M. Synthesis, Structural and Hydrogenation Properties of Mg-Rich MgH_2-TiH_2 Nanocomposites Prepared by Reactive Ball Milling under Hydrogen Gas. *Phys Chem Chem Phys* **2012**, *14*, 1200–1211.
(39) Ponthieu, M.; Calizzi, M.; Pasquini, L.; Fernandez, J. F.; Cuevas, F. Synthesis by Reactive Ball Milling and Cycling Properties of MgH_2-TiH_2 Nanocomposites: Kinetics and Isotopic Effects. *Int J Hydrogen Energy* **2014**, *39*, 9918–9923.
(40) Ponthieu, M.; Cuevas, F.; Fernandez, J. F.; Laversenne, L.; Porcher, F.; Latroche, M. Structural Properties and Reversible Deuterium Loading of MgD_2-TiD_2 Nanocomposites. *J Phys Chem C* **2013**, *117*, 18851–18862.
(41) Asano, K.; Enoki, H.; Akiba, E. Synthesis of HCP, FCC and BCC Structure Alloys in the Mg-Ti Binary System by Means of Ball Milling. *J Alloy Compd* **2009**, *480*, 558–563.
(42) Asano, K.; Enoki, H.; Akiba, E. Synthesis of Mg-Ti FCC Hydrides from Mg-Ti BCC Alloys. *J Alloy Compd* **2009**, *478*, 117–120.
(43) Asano, K.; Kim, H.; Sakaki, K.; Page, K.; Hayashi, S.; Nakamura, Y.; Akiba, E. Synthesis and Structural Study of Ti-Rich Mg-Ti Hydrides. *J Alloy Compd* **2014**, *593*, 132–136.
(44) Liang, G.; Schulz, R. Synthesis of Mg-Ti Alloy by Mechanical Alloying. *J Mater Sci* **2003**, *38*, 1179–1184.
(45) Srinivasan, S.; Magusin, P. C. M. M.; Kalisvaart, W. P.; Notten, P. H. L.; Cuevas, F.; Latroche, M.; van Santen, R. A. Nanostructures of $Mg_{0.65}Ti_{0.35}D_x$ Studied with X-Ray Diffraction, Neutron Diffraction, and Magic-Angle-Spinning ^2H NMR Spectroscopy. *Phys Rev B* **2010**, *81*, 054107–054110
(46) Doppiu, S.; Schultz, L.; Gutfleisch, O. In Situ Pressure and Temperature Monitoring during the Conversion of Mg into MgH_2 by High-Pressure Reactive Ball Milling. *J Alloy Compd* **2007**, *427*, 204–208.
(47) Rodriguez-Carvajal, J. Recent Advances in Magnetic-Structure Determination by Neutron Powder Diffraction. *Physica B* **1993**, *192*, 55–69.
(48) Brinks, H. W.; Fossdal, A.; Bowman, R. C.; Hauback, B. C. Pressure-Composition Isotherms of $TbNiAlH_x$. *J Alloy Compd* **2006**, *417*, 92–95.
(49) Zhang, J. X.; Cuevas, F.; Zaidi, W.; Bonnet, J. P.; Aymard, L.; Bobet, J. L.; Latroche, M. Highlighting of a Single Reaction Path during Reactive Ball Milling of Mg and TM by Quantitative H_2 Gas Sorption Analysis to Form Ternary Complex Hydrides (TM = Fe, Co, Ni). *J Phys Chem C* **2011**, *115*, 4971–4979.
(50) Chen, Y.; Williams, J. S. Formation of Metal-Hydrides by Mechanical Alloying. *J Alloy Compd* **1995**, *217*, 181–184.

(51) Zhang, H.; Kisi, E. H. Formation of Titanium Hydride at Room Temperature by Ball Milling. *J Phys-Condens Mat* **1997**, *9*, L185–L190.
(52) Dunlap, R. A.; Cheng, Z. H.; MacKay, G. R.; O'Brien, J. W.; Small, D. A. Preparation of Nanocrystalline Metal Hydrides by Ball Milling. *Hyperfine Interact* **2000**, *130*, 109–126.
(53) Friedrichs, O.; Sanchez-Lopez, J. C.; Lopez-Cartes, C.; Dornheim, M.; Klassen, T.; Bormann, R.; Fernandez, A. Chemical and Microstructural Study of the Oxygen Passivation Behaviour of Nanocrystalline Mg and MgH_2. *Appl Surf Sci* **2006**, *252*, 2334–2345.
(54) Pearson, W. B. *The Crystal Chemistry and Physics of Metals and Alloys*; Wiley: New York, 1972.
(55) Kuji, T.; Matsumura, Y.; Uchida, H.; Aizawa, T. Hydrogen Absorption of Nanocrystalline Palladium. *J Alloy Compd* **2002**, *330*, 718–722.
(56) Ares, J. R.; Cuevas, F.; Percheron-Guegan, A. Mechanical Milling and Subsequent Annealing Effects on the Microstructural and Hydrogenation Properties of Multisubstituted $LaNi_5$ Alloy. *Acta Mater* **2005**, *53*, 2157–2167.
(57) Jensen, I. J. T.; Diplas, S.; Lovvik, O. M. Hydrogen Induced Stabilization of Meta-Stable Mg-Ti. *Appl Phys Lett* **2012**, *100*, 111902–111904.